Macromolecular Bioscience
www.mbs-journal.de

Guided Cell Attachment via Aligned Electrospinning of Glycopolymers

Renjie Liu, Caglar Remzi Becer, and Hazel R. C. Screen**

The creation of biomaterials with aligned fibers offers broad applications in tissue regeneration, guiding cell organization and physiological cues, and providing appropriate mechanical properties for many biomedical applications. Herein, for the first time, highly aligned electrospun membranes are designed and developed using glycopolymers. The membranes retain the strong mechanical properties of polycaprolactone, and fiber alignment facilitates the creation of anisotropic mechanical properties, enabling failure stress to be manipulated by an order of magnitude relative to randomly ordered fibers. Biocompatibility and cell attachment in these materials are characterized using tenocytes as a cell model. Both random and aligned fiber glycopolymers show promising biocompatibility, but aligned glycopolymer fibers additionally offer patterning to guide cell organization. These materials potentially provide a novel platform for tissue regeneration studies, demonstrating that the sugar–lectin interaction can produce materials capable of managing cell guidance.

1. Introduction

Tissues such as tendon,[1] intervertebral disc,[2] or artery[3] have a 3D hierarchical structure in which mechanical integrity is generally provided by collagen, arranged into fibrils or fibers, with a size range from nanometers to millimeters. Fibrous nano and microscale 3D scaffolds have subsequently been extensively used to mimic the matrix of human tissue for biological applications, such as providing scaffolds for repair.[4] However, the healing of tissues in which the fibers are highly organized can be challenging, as the injury site is generally poorly organized, comprising less dense and disorganized collagen.[5,6] In most cases, poor healing will lead to reduced mechanical properties of the tissue, and an inability to withstand high forces, either reinjuring the same site, or even inducing a second injury.[7,8]

The production of aligned fibrous scaffolds able to recapitulate the anisotropic tensile strength of tissue has received considerable interest as a mechanism of supporting the repair of aligned fibrous tissues. However, it is crucially important that such a scaffold can also provide appropriate cellular cues. In many instances, collagen has been used directly to fabricate scaffolds.[9,10] However, while cell attachment is excellent in collagen scaffolds, their poor structural stability limits their practical application.[11] Previous studies have shown that by aligning fibers in naturally derived materials such as cellulose[12,13] or chitosan-based[14] materials, cell adhesion and alignment can be controlled to recapitulate the direction of fiber alignment, while providing structural stability also. However, the high stiffness and low flexibility of these materials have limited their adoption for biomedical applications.

With the recent developments in polymer chemistry, synthetic biodegradable polymers have gained increasing interest in the last few years.[15] Among the biodegradable candidates, poly (ε-caprolactone) (PCL) has been of particular prominence, due to its excellent biocompatibility and sustained biodegradable duration.[16] Furthermore, PCL can be processed via electrospinning, offering a straightforward mechanism for arranging the fiber orientation.[17]

However, PCL-based materials are commonly restricted in use, owing to their lack of functional groups, providing poor interaction with cells, further exacerbated by the hydrophobic nature of the polymer. Looking to address this, we previously developed a glycopolymer, manufactured as an electrospun membrane, in which the addition of sugar was shown to significantly improve the interaction between the PCL and tenocytes.[18]

The development of synthetic polymer chemistry provides the possibility to design functionalized macromolecules and fabricate materials with desired properties. Numerous polymers with sophisticated structures, for instance, block copolymers, sequence-controlled polymers, and miktoarm polymers, have been designed and synthesized. Among these new structures, block copolymers have been utilized to fabricate nanoparticles,[19,20] because of their self-assembly property, while miktoarm polymers combine the merits of different polymerization techniques with the ability to use materials with advanced properties, such as targeting and loading properties.[21,22] These benefits have drawn considerable interest from the biological community.

R. Liu, Dr. C. Remzi Becer
Polymer Chemistry Laboratory
School of Engineering and Materials Science
Queen Mary University of London
E1 4NS London, UK
E-mail: r.becer@qmul.ac.uk
Prof. H. R. C. Screen
Institute of Bioengineering
School of Engineering and Materials Science
Queen Mary University of London
E1 4NS London, UK
E-mail: h.r.c.screen@qmul.ac.uk
The ORCID identification number(s) for the author(s) of this article can be found under https://doi.org/10.1002/mabi.201800293.

DOI: 10.1002/mabi.201800293

In this study, we further utilize a PCL-containing miktoarm glycopolymer, investigating the capacity to control membrane mechanical properties and manipulate cell attachment and organization, by altering fiber alignment. Electrospun membranes with different fiber alignment and chemical composition were fabricated. Excitingly, our study shows that aligned fiber membranes offer a platform with increased mechanical properties and cell attachment patterns physiologically appropriate for tissue repair.

2. Experimental Section

2.1. Materials

Ethidium homodimer was purchased from Sigma-Aldrich while DMEM, Dulbecco's phosphate-buffered saline, MEM nonessential amino acids, *N*-2-hydroxyethylpiperazine-*N*-2-ethane sulfonic acid (HEPES), L-glutamine, Alexa Fluor 488 Phalloidin, 4′,6-diamidino-2-phenylindole, and dihydrochloride (DAPI) were purchased from Thermo Fisher and used as received. Calcein AM was purchased from Biotium and used as received.

High-molecular-weight homopolymer of PCL (Capa 6500D) was kindly provided by Perstorp Winning Formulas Corporation. Poly(ε-caprolactone)-*mikto*-polystyrene (PCL-*mikto*-PS), Poly(ε-caprolactone)-*mikto*-poly(2,3,4,5,6-pentafluorostyrene) (PCL-*mikto*-PPFS), and Poly(ε-caprolactone)-*mikto*-4-(1-thio-β-D-glucopyranosido)-2,3,5,6-tetrafluorostyrene) (PCL-*mikto*-PTFSGlc) were synthesized and purified as described in our previous published work and used as obtained,[18] the detailed composition of the block copolymers could be found in **Figure 1** and Table S1, Supporting Information.

All other reagents and solvents were purchased from Sigma-Aldrich or Fisher Scientific at the highest purity available and used without further purification unless stated otherwise.

2.2. Preparation of Polymer Electrospinning Solution

Previously synthesized PCL-*mikto*-PS and PCL-*mikto*-PPFS were dissolved in $CHCl_3$: DMF (w/w = 1:3) while PCL-*mikto*-PTFSGlc was dissolved in Ethyl formate: DMF (w/w = 1:3) together with PCL (Capa 6500D) in 20% weight ratios as outlined in **Table 1** following our previous procedures.[18] The solutions were stirred for at least 6 h to achieve a homogenous mixture before electrospinning into membranes.

2.3. Electrospinning of Miktoarm Polymers

Each polymer blend solution was electrospun in turn as described previously[18] (Figure 1b,c). To briefly recap, the polymer solutions were transferred to a plastic syringe (5 mL, Injekt, Braun, Germany) fitted with a metal syringe needle (0.8 mm diameter), and then connected with a 20-gauge polytetrafluoroethylene (PTFE) syringe tube onto the programmable pump (Genie, Kent Scientific Corporation, USA), in which flow rate could be controlled. All membranes were electrospun at 25 kV, supplied directly from a high DC voltage power supply (0–30 kV, Glassman High Voltage, Inc., Whitehouse Station, NJ) with a fixed solution flow rate of 1 mL per hour. The resulting membranes were collected onto either a static aluminum foil-covered steel plate (randomly aligned membranes) or a rotating aluminum foil-covered steel collector (aligned membranes) with a distance between 10 and 15 cm away from the tip of the spinneret. In total, three aligned and three random membranes, approximately 300 mm × 200 mm in size, were made from each sample solution (P1 to P4) and dried in a vacuum at 40 °C overnight to remove the residual solvent before further analysis.

2.4. Surface Analysis of Polymer Membranes

Electrospun membrane morphologies were evaluated using scanning electron microscopy (Inspect F, FEI, The Netherlands), to analyze a 5 mm diameter circular disc punched from each sample. The average fiber diameter of each electrospun membrane was obtained by manually measuring the diameters of at least 100 fibers using Image J (ImageJ software, NIH Image, MD, USA), from at least three SEM images randomly located across the disc and presented as a single value (mean ± standard deviation (SD)).

Surface wettability was also determined via water contact angle measurements (WCA) by depositing a drop of purified water onto the samples utilizing a micro-pipette. A small rectangle sample (20 mm × 30 mm) was cut from each membrane and water drops imaged with a Kruss DSA100 (Hamburg, Germany) followed by image analysis of the sessile drop, using the inbuilt DSA 1.9 software. For each rectangular test piece, at least five measurements were taken at different locations across the surface area.

2.5. Uniaxial Tensile Tests on Electrospun Fibers

All mechanical testing was performed using an Instron 3365 (Instron Co, Norwood, MA, USA) materials testing system at room temperature, equipped with a 100 N load cell. Rectangular samples (40 mm × 10 mm) were prepared manually from P1–P4 membranes, ensuring that samples both with and against fiber direction were prepared from aligned materials. The thickness of each individually prepared sample was measured at least five points along the length using a light microscopy and the mean value used for cross-sectional area calculations. Each test specimen was mounted vertically between the pneumatic grips at a gauge length of roughly 20 mm, after which a 0.1 N preload was applied to ensure a consistent starting condition and then the test gauge length measured. Samples were pulled to failure at 1% strain s^{-1} and the ultimate tensile stress, strain, and modulus were obtained from the calculated stress–strain curves. At least six samples were tested for each type of membrane and fiber orientation condition, and mean values presented.

2.6. Cyclic Recovery Tests on Fibers

The cyclic load response of samples was also investigated, focusing on the P4-A samples, loaded in the fiber direction

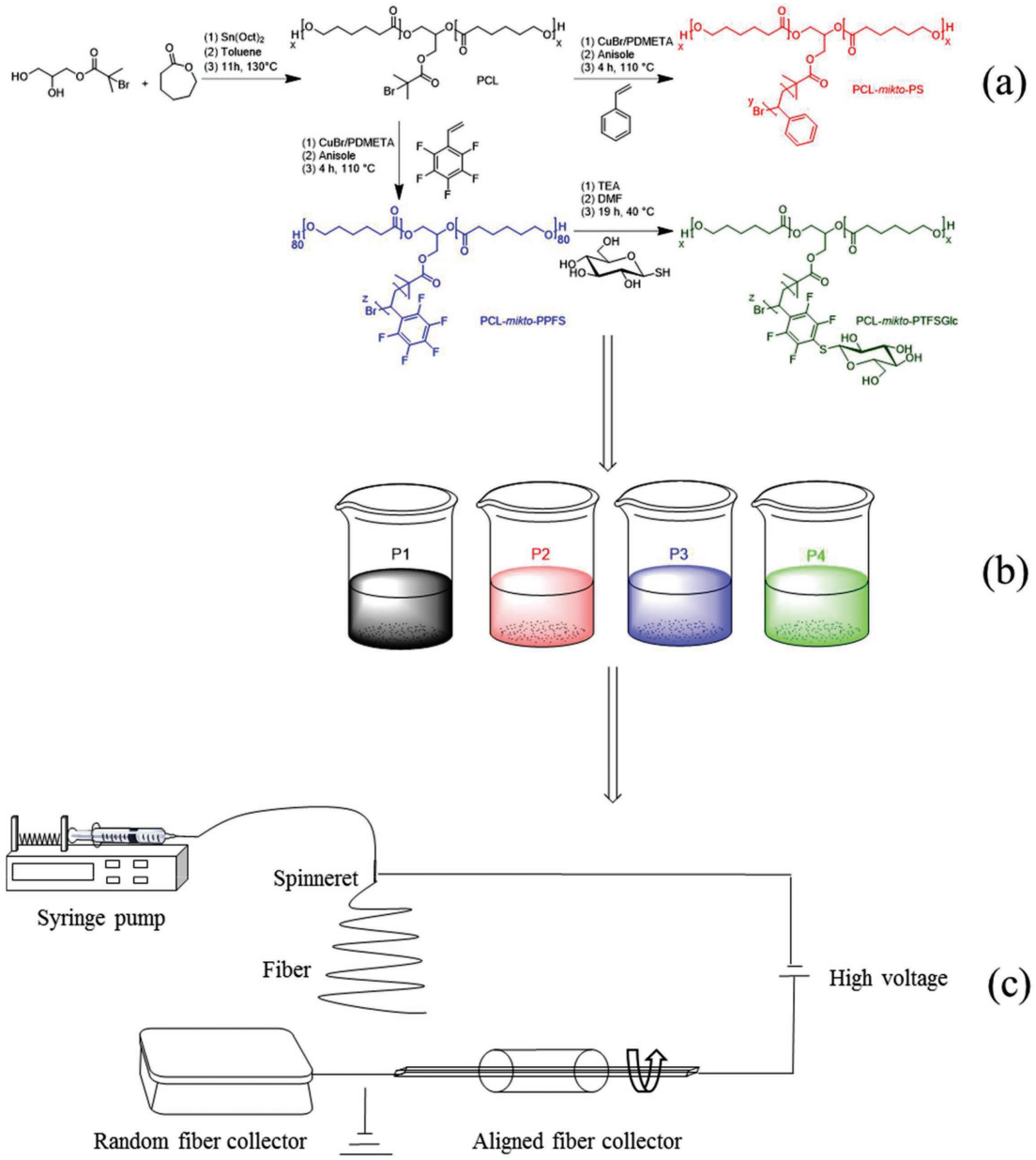

Figure 1. Schematic representation of a) the synthesis of PCL, block copolymers PCL-mikto-PS, PCL-mikto-PPFS, and PCL-mikto-PTFSGlc by ROP of ε-CL and atom transfer radical polymerization (ATRP) of styrene or PPFS and thiol-ene click reaction with thio-glucose, b) electrospun solution preparation, and c) electrospinning setup for membranes with different fiber orientations.

of interest. Samples were prepared, secured in grips, and subjected to a tare load as previously described, after which ten loading-unloading cycles were applied, straining the samples along the fiber direction to either 10%, 20%, and 30% strain (n = 2 per strain condition).[23,24] Samples were then returned to 0% strain for 30 min to allow for any recovery, after which they were subjected to a further ten loading-unloading cycles to the same peak strain, followed by a pull to failure test at 1% strain s^{-1}. The ultimate tensile stress, strain, and modulus were obtained from the pull to failure test, and hysteresis and percentage recovery were calculated from the loading cycles.

2.7. In Vitro Assays on Cell–Biomaterial Interactions

Twelve circular discs (15 mm diameter) were prepared from the residual pieces of each membrane and sterilized by immersion in 70% ethanol overnight followed by 2 h UV light irradiation. All samples were repeatedly washed with sterilized PBS to remove leftover ethanol prior to cell seeding.

Tenocytes were isolated from bovine extensor tendons via tissue digestion (1 U mL^{-1} dispase and 2 mg mL^{-1} collagenase type II for 24 h at 37 °C) and were applied here as a cell source.[25] Tenocytes were cultured in Dulbecco's Modified Eagle Medium (DMEM) (low glucose, pyruvate) containing

Table 1. Composition of solutions for electrospun membranes.

Membrane code	Solution composition	Solvent ratio
Random P1 (P1-R)	PCL[a)]	$CHCl_3$: DMF (w/w = 1:3)
Aligned P1 (P1-A)		
Random P2 (P2-R)	PCL-*mikto*-PS: PCL[a)] = (w/w = 1:4)	$CHCl_3$: DMF (w/w = 1:3)
Aligned P2 (P2-A)		
Random P3 (P3-R)	PCL-*mikto*-PPFS: PCL[a)] = (w/w = 1:4)	$CHCl_3$: DMF (w/w = 1:3)
Aligned P3 (P3-A)		
Random P4 (P4-R)	PCL-*mikto*-PTFSGlc: PCL[a)] = (w/w = 1:4)	Ethyl formate: DMF (w/w = 1:3)
Aligned P4 (P4-A)		

[a)]PCL was kindly provided by Perstorp Winning Formulas Corporation (Capa 6500D).

10% bovine serum, 100 U mL^{-1} penicillin (Life Technologies, Paisley, UK), 1% v/v nonessential amino acids, 2% v/v *N*-2-hydroxyethylpiperazine-*N*-2-ethane sulfonic acid (HEPES), and 1% v/v L-glutamine, at 37 °C, 5% CO_2 in a humidified incubator, and the culture medium was changed every 2 days until harvested at passage 3 using trypsin-EDTA (0.25% trypsin) for further use following the procedures reported before.[18]

2.8. Cell Viability and Affinity on Membranes

Cell affinity and viability on membranes were measured using a live–dead assay, as reported in our previous research.[18] Briefly, six sterilized discs from each group (P1–P4; aligned and random) were aseptically placed into the wells of a non-cell culture-treated 24-well plate, then seeded directly with 2×10^4 cells in 100 µL cell culture medium. Providing controls, 2×10^4 cells in 100 µL cell culture medium were also pipetted onto 6 PEG-containing membranes in non-cell culture-treated plates, and onto six standard cell culture-treated wells in 24-well plates. All 24-well plates were then kept at 37 °C, 5% CO_2 in a humidified incubator in complete culture medium for up to 48 h.

All samples and controls were prepared for imaging at both 24 and 48 h. In brief, 2 µM mL^{-1} calcein AM and 10 µM mL^{-1} ethidium homodimer were added to each well and incubated at 37 °C for 30 min. Membranes were then isolated and observed utilizing a Leica fluorescence microscope (Leica DM4000 B LED, Heidelberg, Germany) under 10× magnification. Samples were imaged, in which calcein AM produced an intense uniform green fluorescence in the cytoplasm of live cells while ethidium homodimer produced a bright red fluorescence in the nucleus of dead cells. A minimum of three pictures were taken at different locations on the surface of each disc at each time point. All pictures were counted in Image J (ImageJ software, NIH Image, MD, USA) to obtain the overall number of live cells (L_m) and dead cells (D_m) on the membrane disc, and live cells (L_w) and dead cells (D_w) in the well.

$$\text{Live cell ratio} = \frac{L_m + L_w}{L_m + L_w + D_m + D_w} \quad (1)$$

Cell viability on membranes was evaluated by calculating the live cell ratio utilizing Equation (1) and compared with positive and negative controls. Furthermore, cell affinity with each material was explored by counting the number of viable cells on each membrane and compared with the number of cells on both positive and negative controls. Cell affinity and viability experiments and analyses were all repeated three times with tenocytes from three different bovine donors and mean data combining all three repeats presented.

2.9. In Vitro Cell Adhesion and Morphology of Cells

Cell adhesion and morphology on membranes were investigated through imaging of the cytoskeleton.[18] Six sterilized discs from each group (P1–P4; aligned and random) and six media-coated glass slides (positive controls) were aseptically placed into the wells of non-treated 24-well plates and seeded directly with 8×10^4 cells in 100 µL cell culture medium. All plates were kept at 37 °C, 5% CO_2 in a humidified incubator in culture medium for up to 48 h, with samples image at 24 and 48 h ($n = 3$ per time point).

To prepare for imaging, samples were washed twice with sterilized PBS, fixed with 4% PFA for 10 min, and then washed again with PBS. The cells were permeabilized with 0.1% Triton X-100 PBS for 5 min followed by further PBS washing, then the actin cytoskeleton stained with 20 µg mL^{-1} Alexa Fluor 488 phalloidin in 1% (wt) bovine serum albumin PBS solution was for 30 min and subsequently washed twice with PBS. Nuclei were also stained with 1 µg mL^{-1} DAPI in 1% (wt) bovine serum albumin PBS solution for 1 min before a final wash in PBS, after which membranes were mounted and imaged employing a Leica confocal laser scanning microscope (Leica TCS SP2; Leica Microsystems, Heidelberg, Germany). A minimum of three pictures were taken at different locations on the surface of each sample at 40× magnification, after which an additional image to elucidate the morphology of a single cell was acquired with a 4× digital zoom.

Confocal images were analyzed using a fast Fourier transform (FFT) as described previously,[26] to elucidate the correlation between fiber alignment and cell orientation presented in the input image. A frequency distribution histogram of fiber direction was established using the directionality plugin in Fiji/ImageJ (ImageJ software, NIH Image, MD, USA),[27] reporting data from –90° to 90° in bins of 2° with 0° degree denoting the mean cell orientation.

The experiment was repeated three times with tenocytes from three different bovine donors and mean data combining all three repeats presented.

2.10. Statistical Analysis

All data were analyzed using statistical analysis software GraphPad Prism 6.0 (GraphPad Software, San Diego, CA, USA) and expressed as mean ± SD. ANOVAs with Tukey comparison of means were performed for live cell ratio and viable number comparison with $p < 0.05$ was considered significant. All the mechanical results were smoothed using Curve Fitting Toolbox

(MATLAB and Statistics Toolbox Release 2017b, The MathWorks, Inc., Natick, MA, USA) to remove noise from the data before further analysis. Due to the non-normal distribution of the mechanical data, Kruskal–Wallis tests were performed followed by Dunn's tests to all mechanical data analysis with $p < 0.05$ considered significant.

3. Results and Discussion

Previously, we have developed a novel synthetic route for the preparation of A_2B-miktoarm polymers and obtained preliminary results on their interaction with tenocytes.[18] Incorporation of sugar moieties promoted tenocyte attachment to materials, potentially through the interaction between sugar moieties and C-type lectins on cells, maintaining good viability, thus showing potential for utilizing these materials in tissue engineering. Synthetic polymers are a common focus for tissue regeneration applications, as the materials offer mechanical stability and thus excellent control of mechanobiology within the systems. PCL has previously been shown to possess stronger mechanical behavior and better stability than other polyesters;[28] however, its interaction with cells is poor and limiting its use in many biological applications.

As one of abundant compound in nature and due to the importance of polymeric carbohydrates in living organisms, glycopolymers are promising candidates to address these limitations through the introduction of sugar moieties into polymer backbone.[29–31] This gives an opportunity to combine the versatility of polymer chemistry with improved cell interaction for biological applications.[32,33] Studies have demonstrated that glycopolymers offer significantly lower toxicity for mammalian cells than standard polymer-based nanoparticles.[34,35]

However, to date, there has been very little work focused on fabricating synthetic glycopolymer-based materials, and the main focus of available studies has been to exploit the properties of the sugar–lectin interactions as a mechanism to isolate or selectively culture a specific cell type from a heterogeneous population[36,37] or to facilitate enzyme immobilization for delivery purpose.[38] Here for the first time, we report the fabrication of aligned glycopolymer-based electrospun membranes, investigating their mechanical behavior in detail, and presenting that they can successfully provide cell guidance over tenocytes.

3.1. Structural Characterization of Polymer Membranes

All membranes (materials P1–P4, aligned and random) appeared to possess a smooth finish when viewed at the macroscale, while individual fiber arrangement was visible at the microscale with scanning electron microscopy. Three images were taken at the microscale to investigate fiber morphology in each membrane, with a representative image of each membrane shown in **Figure 2**. The fiber diameter distribution and mean fiber diameter across all images for each membrane were analyzed and are shown below the corresponding typical image. Fiber diameter ranged from 0.2–0.4 μm (Figure 2), with no notable differences in fiber diameter between materials, while aligned fiber membranes consistently showed smaller fiber diameters than their randomly distributed counterparts.

Water contact angle data demonstrated that while mixing block copolymers with homo PCL did not significantly influence the average diameter of fibers in electrospun membranes, it did change the hydrophilicity of the surface significantly (Figure 2). The incorporation of a hydrophobic block (PS or PPFS) created a surface, which behaved more hydrophobically (P2–P3) while the incorporation of hydrophilic glycopolymer made the surface more hydrophilic (P4). Aligning fibers within membranes resulted in an insignificant but consistent increase in water contact angle relative to the corresponding randomly oriented fiber materials for each hydrophobic membrane only, while glycopolymer-based membranes retained their hydrophilicity regardless of fiber arrangement.

Electrospinning produced uniform diameter fibers, with some variation in fiber dimensions evident for the different material chemistries investigated, likely a result of the solubility of each polymer type in the co-solvent. Creating aligned or randomly oriented fibers was simply achieved with classical electrospinning approaches. Slightly thinner fibers were attained in aligned membranes compared with the random ones, as a result of the dragging force of the collector, while it was also noted that aligning fibers in the hydrophobic block copolymers (P2-P3) led to a further increase in hydrophobicity, which is likely a result of the better organization and reduced spacing between fibers in aligned materials.

3.2. Mechanical Properties of Electrospun Membranes

Quasi-static mechanical test data highlighted no significant differences in the mechanical properties of the four membrane materials, but a significant, order of magnitude increase in the failure properties and modulus of aligned fibers relative to their randomly oriented counterparts when loaded in the fiber direction (**Figure 3**) and a further reduction in these parameters when loaded against the fibers. Trends in sample-specific and material-mechanical parameters were consistent for all membrane materials, indicating consistent fiber arrangement and spacing between test groups.

Based on our previous data indicating improved cell interaction with the P4 membrane,[18] aligned P4 membranes were further explored to ascertain their elastic, plastic, and time-dependent parameters, and capacity to manage repeated cyclic loading, as required in many biological applications.[39]

The cyclic-loading curves demonstrated the Mullins effect, in that the mechanical response is irreversibly dependent on the maximum load previously encountered, with instantaneous softening occurring if the load is increased beyond its previous all-time maximum value (**Figure 4**, Figure S1, Supporting Information). Concomitant with this behavior, most plastic deformation and energy loss were observed within the first cycle (93% deformation and 71% hysteresis), and the aligned P4 samples demonstrated a stable mechanical state with a low strain modulus of 15 MPa and linear region of modulus of 40 MPa after the first cycle, providing potential suitability for applying this material in tissue engineering. Allowing a 30 min recovery period did little to change these

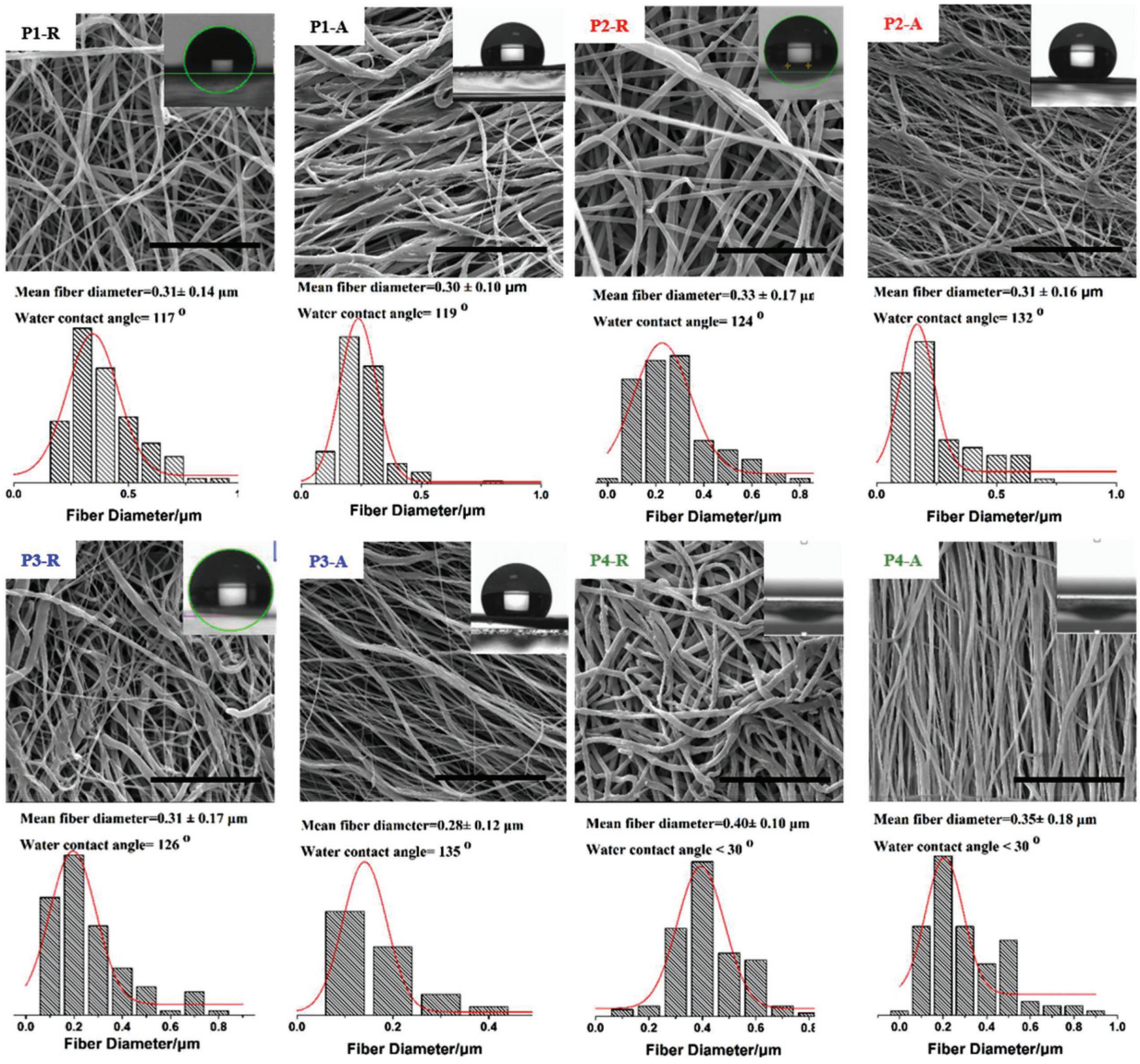

Figure 2. SEM images of both random and aligned polymer membrane of each material (P1–P4), with inset showing the water contact angle result. Mean fiber diameter, mean water contact angle, and frequency distribution of fiber diameter are shown for all images analyzed in each membrane group. Scale bar represents 10 μm in all pictures.

behaviors, and the stable mechanical response was retained (Figure 4b).

One further random and one aligned P4 sample were subjected to ten loading cycles to 30% strain, then prepared for SEM to compare fiber dimensions and alignment after the application of strain (strain applied in the fiber direction where relevant). Three images were taken of the microscale fiber morphology in each membrane, with a representative image of each shown in **Figure 5**. Figure 5 shows no clear change in fiber orientation in either membrane after loading, but does suggest thinning of fiber diameter after loading.

The mechanical properties of the materials were investigated, and as typically seen in aligned fiber systems, significant increases in failure stress and modulus and a reduction in failure strain were seen when materials were loaded in the fiber direction, as the large majority of fibers are directly loaded and recruited to resist the applied strain, with less capacity for fiber reorganization under loading.[40]

Further, while a large energy loss was seen in the first loading cycle for the material, behavior was consistent with further loading, indicating promising mechanical stability. Such "plastic-rubber" behavior is common in PCL-derived materials and other polymers and is commonly referred to as the Mullin's effect.[41] During the first loading cycle, weaker bonds between fiber bundles will start to rupture and thus lead to the softening of the materials, after which stable mechanical behavior will be witnessed with further cycles to the same strain. However, instantaneous softening will appear again if the load is increased beyond its previous all-time maximum value at which point further of the weak bonds can be broken. Interestingly, after 30 min of rest, a small amount of recovery was seen in the loading curve (Figure 4b), which may result from

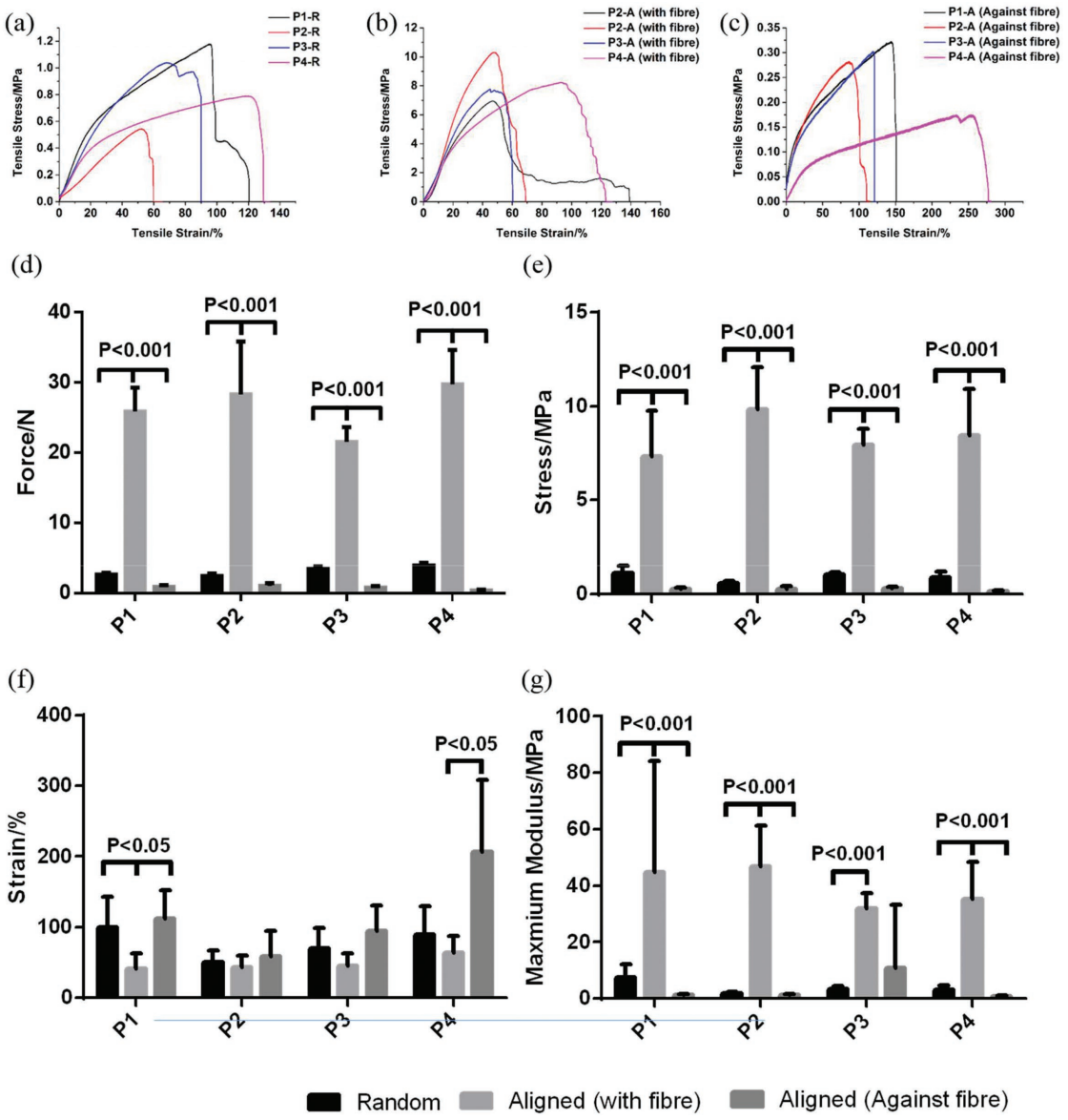

Figure 3. a–c) Representative pull to failure curves for both random and aligned polymer membranes (P1–P4; with and against the fiber). All the samples were pulled to failure at 1% strain s-1. Note the substantial variation of scale on the *y*-axis is required to clearly present the data; d–g) comparison of mean failure force, failure stress, failure strain, and maximum modulus between each random and aligned polymer membrane group. Values represent the mean ± SD ($n = 6$). Statistical significance was calculated using the Kruskal–Wallis tests followed by Dunn's tests method. No significant differences were evident between the different materials.

the movement of polymer chains above their glass transition temperature, leading to the rebuild of bonds between fibers. Further investigation of these relationships is warranted to fully understand material behavior.

Relating these mechanical parameters to those of other scaffold materials, or typical aligned fibrous tissues, shows promising strength, stability, and flexibility of the glycopolymer membranes.[42] In their stable state, the glycopolymer membranes achieved a modulus of around 40 MPa and failure strain of 40%. This offers vastly improved stiffness and stability relative to typical natural materials such as collagen gels[11] but not at the expense of poor flexibility as seen with cellulose[12,13] or chitosan-based[14] materials. Indeed, the mechanical parameters are reaching those of tendon or ligament, which are generally in the range of ≈500 MPa modulus and 10–25% failure strain.[43–45]

3.3. Results of Cell Viability and Affinity on Membranes

One additional key function of aligned fiber systems in tissue engineering is to guide cell attachment[46] and cell signaling.[47] In tissues with aligned fibers, such as tendon, ligament, and intervertebral disc, cells are generally highly elongated and arranged in rows between fibers, connected via gap junctions along and between rows.[48,49]

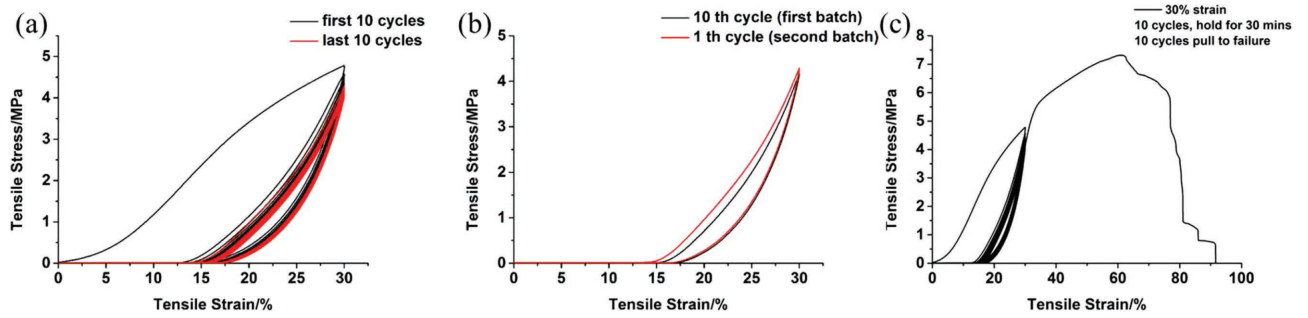

Figure 4. Example cyclic loading curves for aligned P4 samples. Samples were pulled up to 30% strain for ten cycles, held at 0% strain for 30 min, and then pulled to 30% strain at 1% strain s-1 for ten further cycles. a) Stress–strain curves of the first and last ten cycles; b) a direct comparison of the stress–strain curve of the last cycle from first loading batch and the first cycle from the second loading batch; c) representative stress–strain curve, showing cyclic loading followed by pull to failure data, demonstrating a typical Mullins effect.

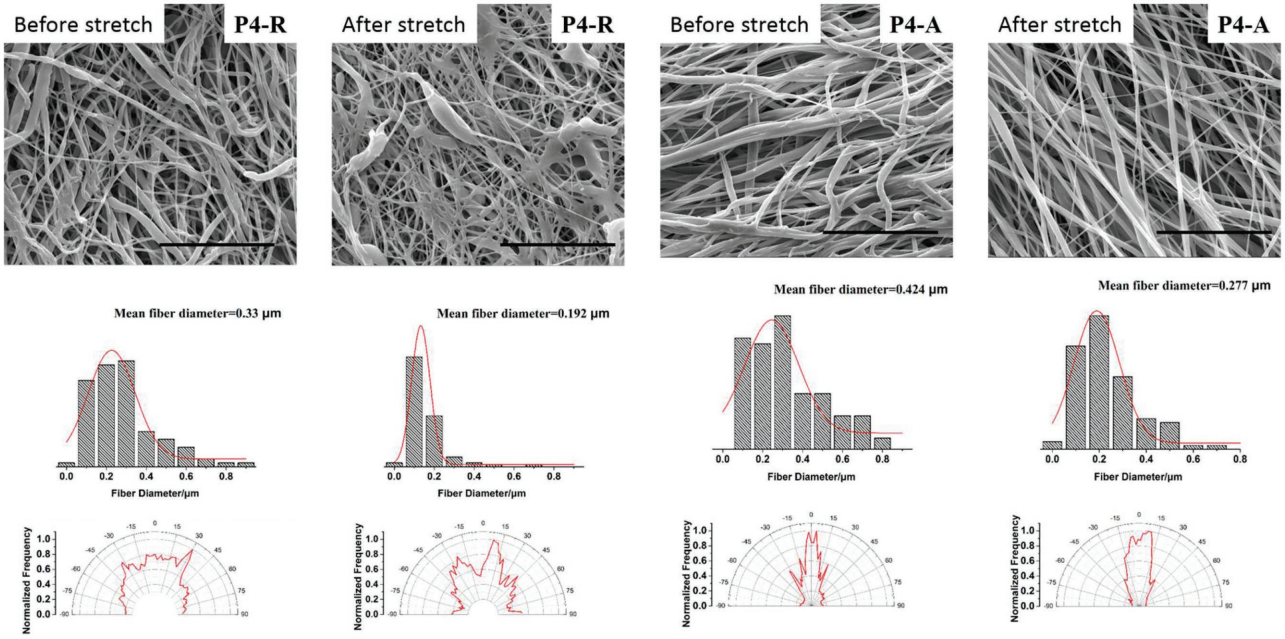

Figure 5. SEM images of both random and aligned polymer membranes before and after ten loading cycles to 30% strain; frequency distributions of fiber diameter and angle plots of fiber alignment are shown for each image. Scale bar represents 10 μm in all pictures.

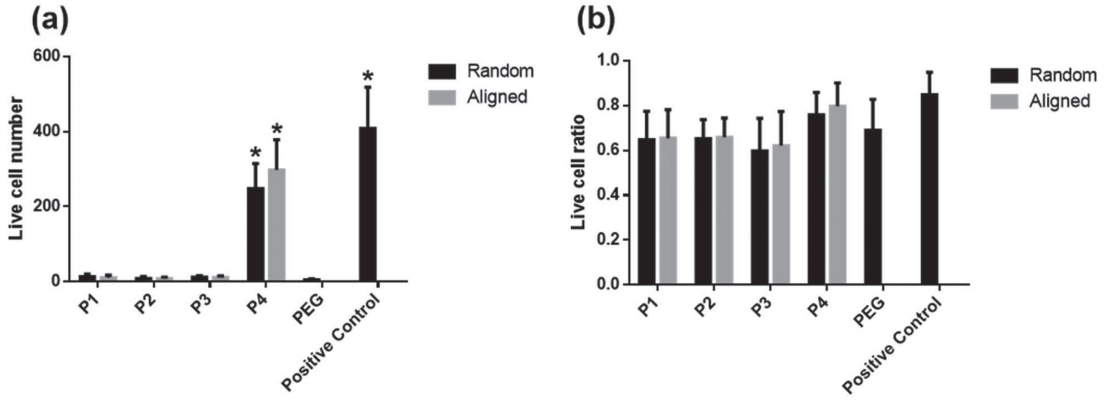

Figure 6. a) Total number of live cells and b) cell viability, as a live:dead ratio, for tenocytes on each of the eight different membrane groups, in comparison with a positive control and a PEG negative control. Values represent the mean ± SD of all samples ($n = 3$). Statistical significance was calculated using a one-way ANOVA followed by Tukey comparison of means method. * = $p < 0.005$. Significantly greater numbers of cell were attached on the P4 membranes than on materials P1–P3.

Live–dead imaging was used to establish overall viable cell numbers and percentage viability at 24 and 48 h on each material (**Figure 6**). Cell viability was maintained above 60% in all test groups for up to 48 h of incubation (Figure 6b), with no significant differences evident between any of the test groups, nor between test groups and a positive control of cells cultured on tissue culture plates.

However, in line with our previous study, viable cell numbers, used here as an indication of cell coverage of a material, were significantly improved on the sugar-incorporating P4

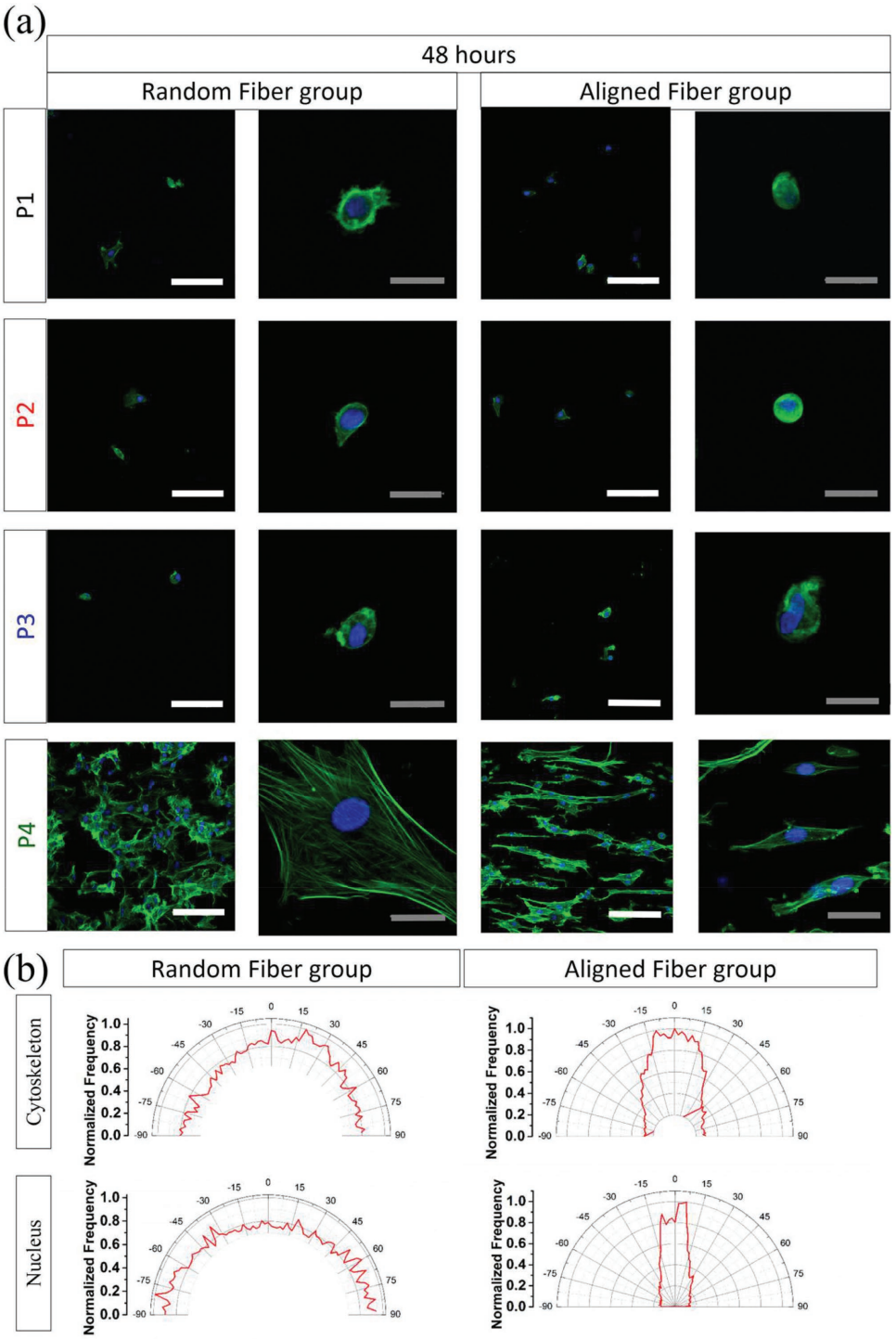

Figure 7. a) Typical confocal images of tenocytes seeded onto both random and aligned polymer membranes (P1 to P4) after 48 h. Green staining represents the cytoskeleton while blue represents the nucleus of cells. Two different magnifications are shown for each condition: the white scale bar represents 100 µm; the gray scale bar represents 25 µm. b) Angle histograms of cell actin (top column) and nucleus (bottom column) orientation distribution on both random and aligned fiber membranes highlight that cells align in parallel rows on the aligned glycopolymer-based membrane P4.

membranes relative to the P1–P3 membranes or a hydrophilic PEG-containing negative control (Figure 6a).

3.4. In Vitro Cell Adhesion and Morphology

The ability of our glycopolymer-based material to control tenocyte organization was subsequently investigated, to determine if in vivo cell organization could be recapitulated. Cytoskeletal imaging demonstrated that in line with our previous findings, tenocytes on the P4 membranes were better adhered, presenting as less rounded cells with a more extensive cytoskeletal network relative to cells on P1–P3 membranes. Concerning those few cells, which did attach to membranes P1–P3, no differences were evident in cell organization in relation to fiber organization. However, cell morphology was notably influenced by fiber organization in the glycopolymer-based material P4. While cells showed a more circular shape and random distribution of stress fibers on randomly organized fiber membranes, the cells were elongated and the cytoskeletal stress fibers consistently aligned parallel with fiber direction on the aligned fibrous membranes at both the 24 and 48 h time points (**Figure 7**, Figures S2 and S3, Supporting Information). Furthermore, the cell nuclei presented as oval in shape, with the long axis also parallel to the fiber direction (Figure 7).

Excitingly, both cytoskeletal stress fibers and the cell nuclei of tenocytes were elongated and aligned parallel to fibers on the aligned glycopolymer membranes (Figure 7, Figures S2 and S3, Supporting Information), recapitulating a number of the key features of cell organization within tissues such as tendon.

While this capacity to control cell organization has previously been demonstrated with peptide functionalized aligned fiber polymers,[50] this is the first time that a synthetic glycopolymer has been shown to exhibit the same effect on cell attachment. Previous studies have demonstrated that synthetic glycopolymers can interact specifically with human C-type lectins[51] and the sequence of sugar moieties diversifies the specific interaction,[52] potentially explain this promising cell–material interaction. However, the mechanisms by which tenocytes interact with glycopolymers needs to be addressed by further study.

4. Conclusion

In summary, we have demonstrated for the first time that PCL- and glycopolymer-based electrospun membranes can be successfully fabricated in an aligned form, with controlled mechanical properties of appropriate magnitude to suit a range of biomedical applications. Fiber orientation has been controlled, offering the capacity to recapitulate the anisotropy of many fibrous tissues, and also acting to guide cell organization in a physiological manner. Such biomaterials offer a real promise as a tissue regeneration platform,[53–55] bringing excellent mechanical properties for functional loading in a highly controllable and tunable material, in which cell–material interactions can also be manipulated to meet the needs of different fibrous tissues, through manipulating material chemistry.

Supporting Information

Supporting Information is available from the Wiley Online Library or from the author.

Acknowledgements

R.L. gratefully acknowledges the financial support from the China Scholarship Council (CSC) and Queen Mary University of London.

Conflict of Interest

The authors declare no conflict of interest.

Keywords

cell alignment, electrospinning, glycopolymer, para-fluoro thiol click reaction, tendon repair

Received: August 3, 2018
Revised: September 17, 2018
Published online: October 15, 2018

[1] H. R. Screen, V. H. Chhaya, S. E. Greenwald, D. L. Bader, D. A. Lee, J. C. Shelton, *Acta Biomater.* **2006**, *2*, 505.
[2] M. Humzah, R. Soames, *Anat. Rec.* **1988**, *220*, 337.
[3] C. Xu, R. Inai, M. Kotaki, S. Ramakrishna, *Biomaterials* **2004**, *25*, 877.
[4] C. J. Bettinger, R. Langer, J. T. Borenstein, *Angew. Chem. Int. Ed.* **2009**, *48*, 5406.
[5] T. W. Lin, L. Cardenas, L. J. Soslowsky, *J. Biomech.* **2004**, *37*, 865.
[6] N. Maffulli, S. W. Ewen, S. W. Waterston, J. Reaper, V. Barrass, *Am. J. Sports Med.* **2000**, *28*, 499.
[7] G. Nourissat, F. Berenbaum, D. Duprez, *Nat. Rev. Rheumatol.* **2015**, *11*, 223.
[8] K. Howell, C. Chien, R. Bell, D. Laudier, S. F. Tufa, D. R. Keene, N. Andarawis-Puri, A. H. Huang, *Sci. Rep.* **2017**, *7*, 45238.
[9] N. Naik, J. Caves, E. L. Chaikof, M. G. Allen, *Adv. Healthcare Mater.* **2014**, *3*, 367.
[10] A. Jean, G. C. Engelmayr, *Adv. Healthcare Mater.* **2012**, *1*, 112.
[11] S. J. Lee, J. Liu, S. H. Oh, S. Soker, A. Atala, J. J. Yoo, *Biomaterials* **2008**, *29*, 2891.
[12] S. Ahn, C. O. Chantre, A. R. Gannon, J. U. Lind, P. H. Campbell, T. Grevesse, B. B. O'connor, K. K. Parker, *Adv. Healthcare Mater.* **2018**, *7*, 1701175.
[13] K. M. Z. Hossain, M. S. Hasan, D. Boyd, C. D. Rudd, I. Ahmed, W. Thielemans, *Biomacromolecules* **2014**, *15*, 1498.
[14] C. Zhang, H. Yuan, H. Liu, X. Chen, P. Lu, T. Zhu, L. Yang, Z. Yin, B. C. Heng, Y. Zhang, *Biomaterials* **2015**, *53*, 716.
[15] T. Sang, S. Li, H.-K. Ting, M. M. Stevens, C. R. Becer, J. R. Jones, *Chem. Mater.* **2018**, *30*, 3743.
[16] F. Qu, J. L. Holloway, J. L. Esterhai, J. A. Burdick, R. L. Mauck, *Nat. Commun.* **2017**, *8*, 1780.
[17] M. Castilho, D. Feyen, M. Flandes-Iparraguirre, G. Hochleitner, J. Groll, P. A. Doevendans, T. Vermonden, K. Ito, J. P. Sluijter, J. Malda, *Adv. Healthcare Mater.* **2017**, *6*, 1700311.
[18] R. Liu, D. Patel, H. R. Screen, C. R. Becer, *Bioconjugate Chem.* **2017**, *28*, 1955.
[19] S. O. Kim, H. H. Solak, M. P. Stoykovich, N. J. Ferrier, J. J. de Pablo, P. F. Nealey, *Nature* **2003**, *424*, 411.

[20] Z. L. Tyrrell, Y. Shen, M. Radosz, *Prog. Polym. Sci.* **2010**, *35*, 1128.
[21] K. Khanna, S. Varshney, A. Kakkar, *Polym. Chem.* **2010**, *1*, 1171.
[22] G. M. Soliman, A. Sharma, D. Maysinger, A. Kakkar, *ChemComm.* **2011**, *47*, 9572.
[23] Y. Si, J. Yu, X. Tang, J. Ge, B. Ding, *Nat. Commun.* **2014**, *5*, 5802.
[24] H. W. Liang, Q. F. Guan, L. F. Chen, Z. Zhu, W. J. Zhang, S. H. Yu, *Angew. Chem., Int. Ed.* **2012**, *51*, 5101.
[25] D. Patel, S. Sharma, S. J. Bryant, H. R. Screen, *Adv. Healthcare Mater.* **2016**, *6*, 1601095.
[26] M. S. Godinho, C. T. Thorpe, S. E. Greenwald, H. R. Screen, *Sci. Rep.* **2017**, *7*, 9713.
[27] J. Schindelin, I. Arganda-Carreras, E. Frise, V. Kaynig, M. Longair, T. Pietzsch, S. Preibisch, C. Rueden, S. Saalfeld, B. Schmid, *Nat. Methods* **2012**, *9*, 676.
[28] J. M. Williams, A. Adewunmi, R. M. Schek, C. L. Flanagan, P. H. Krebsbach, S. E. Feinberg, S. J. Hollister, S. Das, *Biomaterials* **2005**, *26*, 4817.
[29] C. R. Becer, M. I. Gibson, J. Geng, R. Ilyas, R. Wallis, D. A. Mitchell, D. M. Haddleton, *J. Am. Chem. Soc.* **2010**, *132*, 15130.
[30] A. L. Parry, N. A. Clemson, J. Ellis, S. S. Bernhard, B. G. Davis, N. R. Cameron, *J. Am. Chem. Soc.* **2013**, *135*, 9362.
[31] M. Ahmed, R. Narain, *Biomaterials* **2011**, *32*, 5279.
[32] D. Schmaljohann, *Adv. Drug Deliv. Rev.* **2006**, *58*, 1655.
[33] K. Rezwan, Q. Chen, J. Blaker, A. R. Boccaccini, *Biomaterials* **2006**, *27*, 3413.
[34] V. P. Narayanaswamy, S. A. Giatpaiboon, J. Uhrig, P. Orwin, W. Wiesmann, S. M. Baker, S. M. Townsend, *PLoS One* **2018**, *13*, e0191522.
[35] D. Pranantyo, L. Q. Xu, Z. Hou, E.-T. Kang, M. B. Chan-Park, *Polym. Chem.* **2017**, *8*, 3364.
[36] Q. Meng, A. Haque, B. Hexig, T. Akaike, *Biomaterials* **2012**, *33*, 1414.
[37] C. Zhao, Q. Shi, J. Hou, Z. Xin, J. Jin, C. Li, S.-C. Wong, J. Yin, *J. Mater. Chem. B* **2016**, *4*, 4130.
[38] J. Quan, Z. Liu, C. Branford-White, H. Nie, L. Zhu, *Colloids Surf., B* **2014**, *121*, 417.
[39] S. Teoh, *Int. J. Fatigue* **2000**, *22*, 825.
[40] B. Xu, W. D. Cook, C. Zhu, Q. Chen, *Polym. Int.* **2016**, *65*, 423.
[41] R. R. Duling, R. B. Dupaix, N. Katsube, J. Lannutti, *J. Biomech. Eng.* **2008**, *130*, 011006.
[42] B. Chan, K. Leong, *Eur. Spine J.* **2008**, *17*, 467.
[43] G. A. Johnson, D. M. Tramaglini, R. E. Levine, K. Ohno, N. Y. Choi, S. L-Y. Woo, *J. Orthop. Res.* **1994**, *12*, 796.
[44] C. T. Thorpe, H. L. Birch, P. D. Clegg, H. R. Screen, *Int. J. Exp. Pathol.* **2013**, *94*, 248.
[45] C. Thorpe, H. Birch, P. Clegg, H. Screen, *Osteoarthr. Cartil.* **2012**, *20*, S246.
[46] S.-H. Park, M. S. Kim, B. Lee, J. H. Park, H. J. Lee, N. K. Lee, N. L. Jeon, K.-Y. Suh, *ACS Appl. Mater. Interfaces* **2016**, *8*, 2826.
[47] S. Y. Chew, R. Mi, A. Hoke, K. W. Leong, *Biomaterials* **2008**, *29*, 653.
[48] S. C. Juneja, *J. Tissue Eng.* **2013**, *4*, 204173141349274.
[49] A. Maroudas, R. Stockwell, A. Nachemson, J. Urban, *J. Anat.* **1975**, *120*, 113.
[50] D. Grafahrend, K.-H. Heffels, M. V. Beer, P. Gasteier, M. Möller, G. Boehm, P. D. Dalton, J. Groll, *Nat. Mater.* **2011**, *10*, 67.
[51] G. Yilmaz, C. R. Becer, *Polym. Chem.* **2015**, *6*, 5503.
[52] C. Lavilla, G. Yilmaz, V. Uzunova, R. Napier, C. R. Becer, A. Heise, *Biomacromolecules* **2017**, *18*, 1928.
[53] S. Quan, P. Kumar, R. Narain, *ACS Biomater. Sci. Eng.* **2016**, *2*, 853.
[54] G. Zhao, X. Zhang, T. J. Lu, F. Xu, *Adv. Funct. Mater.* **2015**, *25*, 5726.
[55] S. Y. Chew, R. Mi, A. Hoke, K. W. Leong, *Adv. Funct. Mater.* **2007**, *17*, 1288.